Chlorophyll

Deutsche Ausgabe: DOI: 10.1002/ange.201512001
Internationale Ausgabe: DOI: 10.1002/anie.201512001

Fine Tuning of Chlorophyll Spectra by Protein-Induced Ring Deformation

*Dominika Bednarczyk, Orly Dym, Vadivel Prabahar, Yoav Peleg, Douglas H. Pike, and Dror Noy**

Abstract: *The ability to tune the light-absorption properties of chlorophylls by their protein environment is the key to the robustness and high efficiency of photosynthetic light-harvesting proteins. Unfortunately, the intricacy of the natural complexes makes it very difficult to identify and isolate specific protein–pigment interactions that underlie the spectral-tuning mechanisms. Herein we identify and demonstrate the tuning mechanism of chlorophyll spectra in type II water-soluble chlorophyll binding proteins from Brassicaceae (WSCPs). By comparing the molecular structures of two natural WSCPs we correlate a shift in the chlorophyll red absorption band with deformation of its tetrapyrrole macrocycle that is induced by changing the position of a nearby tryptophan residue. We show by a set of reciprocal point mutations that this change accounts for up to 2/3 of the observed spectral shift between the two natural variants.*

Photosynthetic organisms utilize only a few types of pigments for harvesting incoming solar radiation. The versatility of the photosynthetic apparatus, and its robustness to different and variable illumination conditions are achieved by closely packing arrays of pigments, primarily chlorophylls (Chls), bacteriochlorophylls (BChls), and carotene derivatives within protein complexes. The protein environment adjusts the electronic properties of individual pigments by specific protein–pigment interactions that tune their excitation energies. Interactions among the closely spaced Chls lead to a set of delocalized excited states, or excitons. The transition energies of these excitons are controlled by the variations of pigments' local site energies, spatial separation, and relative orientation. This leads to a diverse and tunable excited-states energy landscape that determines the dynamics of excitation energy transfer through the arrays of light-harvesting pigments.[1]

Excitation energy-transfer dynamics in photosynthetic light-harvesting complexes has been extensively studied.[1c,2] Research in the field has benefited from the abundance of protein samples, availability of high-resolution crystal structures of light-harvesting complexes,[3] and the applicability of high time and spectral resolution spectroscopic techniques.[1c,2b,4] This provided plenty of insight into the design principles of natural light harvesting and important lessons on engineering efficient artificial light-harvesting systems. However, the size and complexity of the natural systems that contain many pigments, that are usually strongly coupled, severely limit the means of obtaining information about site energies of individual light-harvesting pigments. These cannot be measured directly and can only be evaluated by theoretical modeling, or by fitting simulated spectra to experimental data.[2a,5] Consequently, identifying and isolating specific protein–pigment interactions that tune the site energies becomes extremely difficult.

Herein, we present a structural and spectroscopic study that elucidates the mechanism of tuning Chl spectra in the type II water-soluble Chl binding proteins from *Brassicaceae* (WSCP). The simple and symmetric structure of these proteins makes them an excellent model system for studying Chl–protein interactions.[6] We focus on the origin of the difference between the lowest energy Qy absorption bands of Chl a in two natural variants of WSCP representing two distinct subclasses of type II WSCP. The first variant, WSCP from cauliflower (CaWSCP) represents type IIa WSCP and is characterized by a Qy peak at 673 nm, whereas the second variant, WSCP from *Lepidium virginicum* (LvWSCP) represents type IIb WSCP and is characterized by a Qy peak at 664 nm. To explain this shift, which corresponds to a site energy difference of 201 cm^{-1}, we employed a novel method based on water-in-oil emulsions for assembling recombinantly expressed apoproteins of WSCP with Chl a.[7] By using this method, we could construct, purify, and solve the crystal structure of CaWSCP-Chl a complex. The structure is highly homologous to the previously elucidated structure of native LvWSCP (PDB ID: 2DRE).[8] Yet, closer inspection reveals significant deformation of the Chl macrocycle planarity in CaWSCP with respect to LvWSCP. This type of deformation is well known to induce a red shift in the Qy absorption bands of Chls, BChls, and other porphyrin derivatives.[9] In WSCP, it is induced by a specific change in the protein environment. Explicitly, a single mutation of asparagine to alanine modifies the hydrogen bonding to a nearby tryptophan residue, which

[*] Dr. D. Bednarczyk
Department of Biological Chemistry, Weizmann Institute of Science
Rehovot (Israel)
Dr. O. Dym, Dr. Y. Peleg
Israel Structural Proteomics Center, Weizmann Institute of Science
Rehovot (Israel)
D. H. Pike
Department of Biochemistry and Molecular Biology and the Center for Advanced Biotechnology and Medicine, Robert Wood Johnson Medical School
Rutgers University
679 Hoes Lane West, Piscataway, NJ 08854 (USA)
Dr. V. Prabahar, Dr. D. Noy
Migal-Galilee Research Institute
S. Industrial Zone, Kiryat Shmona (Israel)
E-mail: drorn@migal.org.il

Supporting information for this article can be found under: http://dx.doi.org/10.1002/anie.201512001.

 © 2016 Wiley-VCH Verlag GmbH & Co. KGaA, Weinheim

brings it closer to the Chl macrocycle and thereby leads to deformation. To verify this mechanism we constructed a set of reciprocal point mutants of CaWSCP and LvWSCP, assembled them with Chl a, and compared their absorption spectra. We show that it is possible to shift the Qy band position back and forth by a single point mutation of alanine to asparagine and vice versa. To our knowledge, this is the first experimental demonstration of spectral tuning that relies exclusively on inducing conformational changes in the Chl macrocycle by its protein environment.

Recombinant CaWSCP was assembled with Chl a by the water-in-oil emulsion method previously developed by us.[7] Purification and crystallization enabled solving the molecular structure of the complex at 1.9 Å resolution (see Supporting Information for more details; the structure's coordinates were deposited in the RCSB Protein Data Bank under accession code 5HPZ). Overall, the structures of recombinant CaWSCP and that of native LvWSCP are very similar (Figure 1). Both assemble as symmetric homotetramers in which each monomeric subunit binds a single Chl. This results in an arrangement of four Chls that is in fact a dimer of excitonically coupled Chl dimers. Overall, the protein structures and Chl arrangements of the monomeric and dimeric subunits of LvWSCP and CaWSCP are highly homologous. But, the interfaces between the dimeric subunits in the tetramer and hence the relative orientation of Chl dimers are not the same.

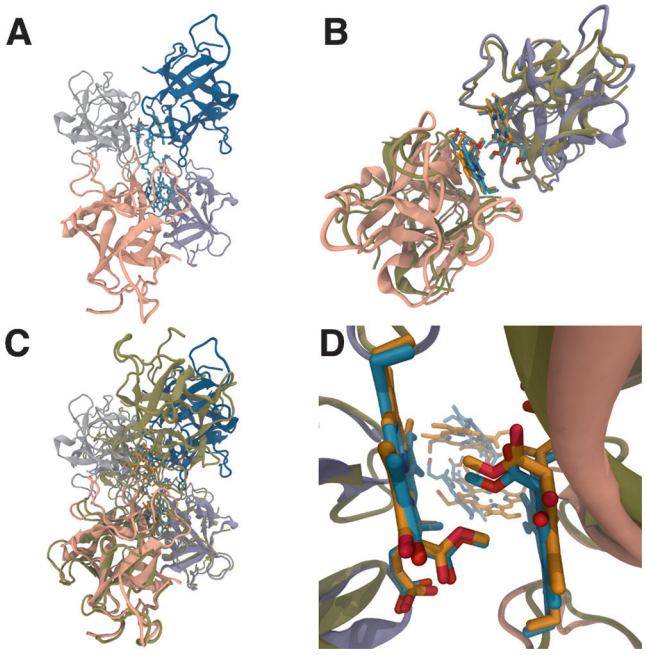

Figure 1. CaWSCP structure and the LvWSCP structure (PDB ID: 2DRE). A) CaWSCP tetramer. Chains A, B, C, and D are purple, pink, gray, and blue, respectively. Chls are shown in stick representation with carbon atoms in cyan. B) Overlay of chains A and B of CaWSCP (same color scheme as in (A)), and LvWSCP shown in brown with Chl carbon atoms in orange. C) Overlay of CaWSCP and LvWSCP (same color scheme as in (A) and (B)). D) A view from chains A and B toward chains C and D of CaWSCP and LvWSCP revealing the rotation of the LvWSCP Chl (orange) dimer with respect to the CaWSCP Chl (cyan) dimer. For clarity, chains C and D, and Chl phytyl chains are not presented. Structures were visualized with VMD.[11]

Aligning the dimeric subunits of CaWSCP and LvWSCP reveals about 60° difference in rotation of one dimeric subunit around the C_2 symmetry axes of the adjacent dimer (Figure 1). However, these variations cannot account for the spectral differences between Chl a in CaWSCP and LvWSCP because the excitonic coupling between the two dimers is too weak to cause any significant change in the absorption spectra.[10]

The shift of the Qy transition energy may arise either from different excitonic interactions between the strongly coupled Chl pairs, or from differences in the protein environment around each Chl.[5a,b] Since the dimer conformations in LvWSCP and CaWSCP are very similar, it is most likely that the shift is due to changes in Chl site energies as a result of Chl–protein interactions. Those interactions known to affect the Chl electronic transitions include 1) axial coordination to the central Mg atom,[5a,12] 2) hydrogen bonding,[13] 3) electrostatic interactions with charged or aromatic residues,[5a,d] and 4) changes in Chl conformation.[9a,14] Inspection and comparison of the Chls and their binding sites reveals that in both CaWSCP and LvWSCP the axial ligand to the Mg atom is the backbone oxygen of a proline residue, the hydrogen bonding network around the acetyl and carbonyl residues of the Chl's rings C and E is highly conserved (Figure 2A), and there are no charged residues within the Chl binding sites of both proteins. A serine at position 84 (S_{84}) in CaWSCP is replaced by alanine at position 87 (A_{87}) in LvWSCP. However, this does not affect the net charge at this position and therefore is unlikely to affect the Chl spectrum in a significant way.

The most significant difference between LvWSCP and CaWSCP appears to be around Chl rings D and A (Figure 2B). An asparagine at position 38 (N_{38}) in LvWSCP is replaced by alanine at position 34 (A_{34}) in CaWSCP. This causes a conserved tryptophan residue (LvWSCP W_{154}, CaWSCP W_{151}) that is hydrogen bonded to the delta-oxygen of N_{38} to form an alternative hydrogen bond with the backbone oxygen of A_{34}. Consequently, the bulky tryptophan sidechain moves away from Chl ring D and closer to Chl ring A, which results in bending the ring out of the Chl macrocycle plain (Figure 2C). In addition, the vinyl group of ring A rotates 180° about the C_3–C_3^1 bond. Mutation of two leucine residues at positions 44 and 91 (L_{44}, and L_{91}) in LvWSCP to phenyl-alanine and valine at positions 40 and 89 (F_{40}, and V_{89}), respectively in CaWSCP accommodate the Chl binding site to the different vinyl group position. AMBER molecular mechanics simulations strongly suggest that the protein conformational changes around the Chl lead to ring deformation (Figure 2D,E). Replacing a Chl in CaWSCP with a planar Chl from LvWSCP and searching for minimal energy conformation of the Chl while keeping all other residues fixed results in a conformation almost identical to that of the original CaWSCP Chl. A similar trend is observed in calculation of the reciprocal case, namely, a bent Chl from CaWSCP in the LvWSCP binding site. The energy-minimized Chl conformation is slightly more planar than the starting point but is still bent. This is most likely due to the minimal energy search converging to a local energy minimum.

© 2016 Wiley-VCH Verlag GmbH & Co. KGaA, Weinheim

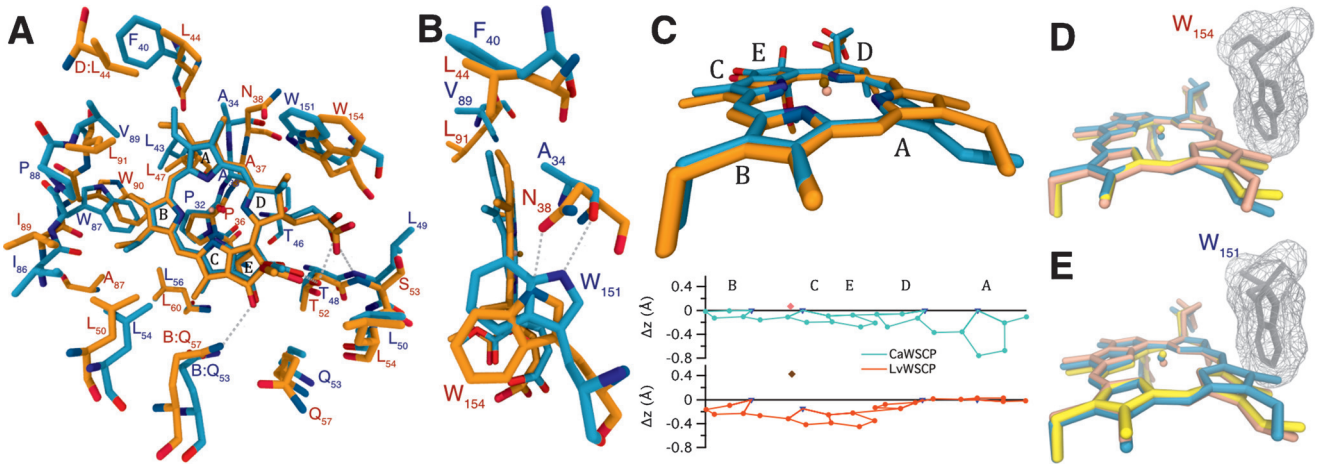

Figure 2. Chl–protein interactions in CaWSCP and LvWSCP. A) Chl and interacting residues. Gray dotted lines represent possible hydrogen bonds. CaWSCP residue labels are blue and LvWSCP residue labels are red. Chl rings are labelled in black according to IUPAC–IUB conventions. B) Amino acids residues interacting with Chl ring A, location of tryptophan and its hydrogen-bonding interactions (dotted lines). C) Deformation of the Chl macrocycle ring represented by comparison of CaWSCP- and LvWSCP-bound Chls aligned at their NA, NB, and NC nitrogen atoms (top), and a plot of displacement of each macrocycle atom from the plane defined by the same nitrogen atoms shown in an (*x*,*z*) projection. For clarity, the *x* coordinates of rings A and D are mirror imaged with respect to the C_{16} carbon atom, and those of rings B, C, and E are shifted by −2.0 Å (bottom). The Mg atoms are marked as diamonds, nitrogen atoms as triangles, and carbon atoms as circles. D) Energy minimization of CaWSCP Chl conformation within the LvWSCP binding site. A Chl from the CaWSCP structure was placed in the LvWSCP Chl binding site (cyan stick representation) and was subject to AMBER molecular mechanics energy minimization. The minimal energy conformation (yellow) and the native LvWSCP Chl structure (pink) are shown in stick representations. E) Energy minimization of LvWSCP Chl conformation within the CaWSCP binding site. A Chl from the LvWSCP structure was placed in the CaWSCP Chl binding site (cyan stick representation) and was subject to AMBER molecular mechanics energy minimization. The minimal energy conformation (yellow) and the native CaWSCP Chl structure (pink) are shown in stick representations. Structures were visualized with VMD.[11]

Ring deformation and vinyl group rotation are known to affect the absorption spectra of Chls.[5b] However, a 180° rotation does not change the conjugation of the vinyl ring to the Chl macrocycle and therefore is not expected to lead to significant spectral variations. By contrast, deformation of the Chl macrocycle is well known to lead to a red shift of the Qy transition in Chls and other porphyrins.[5b,9,14a,15] Thus, it is consistent with the observed red shift in CaWSCP. To verify that the protein conformational changes described above can actually change the Chl spectra, and to quantify the contribution of each amino acid residue to the overall spectral shift, we carried out a set of point mutations in the sequences of LvWSCP and CaWSCP. These included the single mutations N_{38}→A, L_{44}→F, and L_{91}→V in LvWSCP, their reciprocal mutations A_{34}→N, F_{40}→L, and V_{89}→L in CaWSCP, and all possible combinations of double and triple mutations. Altogether, 16 reciprocal mutants (Table 1, and Supporting Information) with single point mutations and combinations of the double and triple amino acid mutations were prepared. Additionally, since CaWSCP's A_{34} and F_{40} as well as LvWSCP's N_{38} and L_{44} residues are at both ends of a seven amino acids loop, we constructed a CaWSCP and a LvWSCP mutant in which the native loops are exchanged (Table 1, Supporting Information). All the apoprotein mutants were assembled in vitro with Chl a, and the absorption spectrum of each protein–pigment complex was recorded.

As expected, the A_{34}→N CaWSCP mutant blue shifts the Chl Qy transition band from 673 nm to 667 nm, whereas the analogous reciprocal N_{38}→A mutation in LvWSCP induces a red shift from 664 nm to 669 nm (Table 1, Figure 3). The other two point mutations in LvWSCP namely, L_{44}→F and L_{91}→V, do not change the Qy band position, but the double mutation induces a blue shift of 1 nm to 663 nm. The reciprocal point mutations in CaWSCP, F_{40}→L, and V_{89}→L induce a 3 nm blue shift and a 1 nm red shift to 670 nm and 674 nm, respectively, whereas the double mutation induces a blue shift of 2 nm to 671 nm (Table 1). Yet, none of the double and triple mutations in CaWSCP, and LvWSCP induces a Qy band shift exceeding that induced by the single mutations A_{34}→N, and N_{38}→A. The only exception is the CaWSCP $A_{34}F_{40}$→$N_{38}L_{44}$ double mutant that blue shifts the Qy band 7 nm to 666 nm. Yet, exchanging the CaWSCP A_{34}-F_{40} loop with LvWSCP's N_{38}-L_{44} loop leads to the same 6 nm blue shift as the A_{34}→N single mutation. The reciprocal

Table 1: Chl Qy absorption peak positions of CaWSCP and LvWSCP mutants.

CaWSCP mutant	Qy peak [nm] (Shift [cm^{-1}])[a]	LvWSCP mutant	Qy peak [nm] (Shift [cm^{-1}])[a]
$A_{34}F_{40}V_{89}$[b]	**673 (−)**	$A_{38}F_{44}V_{91}$	669 (−113)
$A_{34}L_{40}V_{89}$	670 (67)	$A_{38}L_{44}V_{91}$	669 (−113)
$A_{34}L_{40}L_{89}$	671 (44)	$A_{38}L_{44}L_{91}$	669 (−113)
$A_{34}F_{40}L_{89}$	674 (−22)	$A_{38}F_{44}L_{91}$	668 (−90)
$N_{34}F_{40}L_{89}$	667 (134)	$N_{38}F_{44}L_{91}$	664 (0)
$N_{34}F_{40}V_{89}$	667 (134)	$N_{38}F_{44}V_{91}$	664 (0)
$N_{34}L_{40}V_{89}$	666 (156)	$N_{38}L_{44}V_{91}$	663 (23)
$N_{34}L_{40}L_{89}$	667 (134)	**$N_{38}L_{44}L_{91}$**[b]	**664 (−)**
Lv-loop	667 (134)	Ca-loop	668 (−90)

[a] With respect to the native complex. [b] Bold = native sequence.

© 2016 Wiley-VCH Verlag GmbH & Co. KGaA, Weinheim

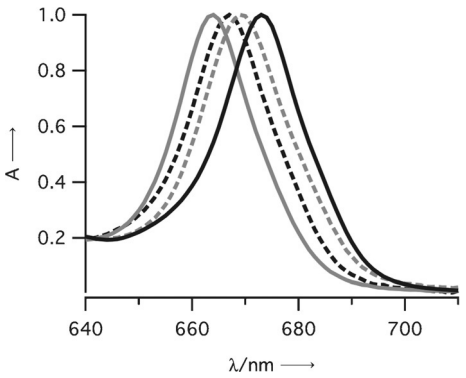

Figure 3. The Qy absorption bands of native CaWSCP (black solid line), and LvWSCP Chl a (gray solid lines), and their respective $A_{34}\rightarrow$N (black dashed line), and $N_{38}\rightarrow$A mutants (gray dashed lines). Spectra were normalized to a Qy absorption peak of 1.0.

mutation in LvWSCP leads to a 4 nm red shift that is 1 nm smaller than the 5 nm red shift of the $N_{38}\rightarrow$A single mutation. Thus, the most significant blue, and red shifts are due to the $A_{34}\rightarrow$N, and $N_{38}\rightarrow$A point mutations and amount to 113 cm^{-1}, and 134 cm^{-1}. This corresponds to 56 %, and 66 % of the total 201 cm^{-1} shift between wild type LvWSCP and CaWSCP, respectively. The extra shift that cannot be accounted for by the specific point mutation may be attributed to a non-specific solvatochromic effect.[5b,16] It is reasonable to assume that the slight variations in protein structure lead to global non-specific differences between CaWSCP and LvWSCP. These vary the local dielectric constant and refractive index around the Chl in each protein, which eventually lead to spectral band shifts.[16b] The mutation $S_{84}\rightarrow$A in CaWSCP led a minor shift of the Qy band to 671 nm, whereas the reciprocal mutation $A_{87}\rightarrow$S in LvWSCP did not have any effect on the Qy band position. This confirms our assumption that this change of polarity by itself is too small to significantly affect the Chl spectra. The overall solvatochromic shift is a cumulative effect of small local variation in polarity, thus it cannot be reproduced by a single point mutation.

Altogether, the set of spectroscopic data from the CaWSCP and LvWSCP mutants confirms our predictions based on the crystal-structure analysis. The ability to shift the Qy band more than 100 cm^{-1} back and forth by changing a single amino acid strongly implicates the repositioning of a tryptophan residue driven by changes in hydrogen bonding to N_{38} or A_{34} as the main cause for the shift. Since the Chl and tryptophan π-systems are almost perpendicular, and the repositioning of the tryptophan π-system does not change significantly the distance between the two π-systems, it is unlikely that direct tryptophan–Chl π–π interactions can lead to a significant Qy band shift. Thus, the most likely cause for Qy band shift is a steric effect of the tryptophan that causes bending of Chl ring A and thereby deformation of the π-system (Figure 2). Such a deviation from macrocycle planarity has been established to cause significant red shifts of the Qy band in porphyrin, Chl, and BChl derivatives.

Ring deformation has long been considered a significant factor affecting the electronic transition energies and redox potentials of porphyrin and chlorin derivatives. As high-resolution structures of Chl proteins become available it is possible to evaluate the effect of Chl ring deformation in actual Chl–protein complexes. Zuccheli et al. rigorously investigated ring deformations in light harvesting complex II (LHCII) by using normal mode structural decomposition analysis,[17] Saito et al.,[18] Jurinovich et al.,[19] and McGowan et al.[20] conducted similar investigations on the Chls and BChls of photosystem II (PSII), and the Fenna–Matthews–Olson (FMO) protein, respectively. Unfortunately, although these surveys revealed a broad range of ring deformations in each complex, the large number of pigments, and their excitonic coupling result in highly congested absorption bands, which prevents straightforward assignments of individual site energies to each (B)Chl and thereby the ability to correlate ring deformations with absorption band shifts. Site-directed mutagenesis, which was employed extensively in the study of LHCII,[12b,21] could modify major Chl–protein contacts, such as axial ligands or hydrogen bonds, as well as eliminate specific Chl binding sites. But the perturbation of neighboring pigments as a result of such drastic modifications has prevented straightforward interpretation of the absorption spectra. Thus, the assignment of transition energies to specific Chl conformations must rely on quantum mechanical calculations. The accuracy of these is still limited by the large size of Chl molecules, which leads to using empirical scaling of the theoretical energies to match the experimental data. These assignment issues are of no concern in the symmetric WSCP tetrameric complex since all four Chl binding sites are equivalent. Thus, variations in site energies in native and mutant WSCPs can be measured and compared directly.

In summary, for the first time, we were able to crystalize and solve a structure of a recombinant WSCP complex reconstituted with Chl a. It is also the first structure of type IIa WSCP. Comparison to type IIb WSCP structure revealed significant Chl-ring deformation, which is well correlated with the 201 cm^{-1} red shift in the Chl Qy transition energy. The deformation is induced by a unique protein conformational change caused by mutation of an asparagine to alanine. This modifies the hydrogen-bonding pattern to a nearby tryptophan, repositioning it closer to the Chl, and causing ring deformation by steric interaction. We verify this mechanism by spectroscopic investigation of a set of reciprocal point mutants showing that the Qy band can be shifted back and forth by up to 134 cm^{-1} by the $A_{34}\rightarrow N/N_{38}\rightarrow$A mutations. This is the only example of tuning Chl spectra by protein-induced ring deformation that can be controlled and monitored directly. It highlights the unique advantages of WSCP as a model system and a spectroscopic benchmark, and opens new possibilities for exploring protein control over Chl site energies in natural light-harvesting complexes and their artificial analogues.

Experimental Section

Complexes of Chls with recombinant WSCP apoproteins were prepared and purified as previously described.[7] Absorption spectra

 © 2016 Wiley-VCH Verlag GmbH & Co. KGaA, Weinheim

were recorded with Jasco V7200 absorption spectrophotometer. Details of WSCP mutant preparation and crystal structure analysis are given as Supporting Information.

Acknowledgements

D.N. acknowledges financial support from the European Research Council (ERC) consolidator grant (GA 615217), and Israel Science Foundation personal grant (GA 558/14). We thank Dr. Alexander Berchansky for critically reading this manuscript and for preparation of the interactive 3D Complement page in Proteopedia, http://proteopedia.org/w/Journal:Angew Chem Int Ed:1

Keywords: chlorophyll · light-harvesting complexes · spectral tuning · water soluble chlorophyll binding protein · structure determination

How to cite: *Angew. Chem. Int. Ed.* **2016**, *55*, 6901 – 6905
Angew. Chem. **2016**, *128*, 7015 – 7019

[1] a) R. Croce, H. van Amerongen, *Nat. Chem. Biol.* **2014**, *10*, 492 – 501; b) G. D. Scholes, G. R. Fleming, A. Olaya-Castro, R. van Grondelle, *Nat. Chem.* **2011**, *3*, 763 – 774; c) Y.-C. Cheng, G. R. Fleming, *Annu. Rev. Phys. Chem.* **2009**, *60*, 241 – 262.

[2] a) V. I. Novoderezhkin, R. van Grondelle, *Phys. Chem. Chem. Phys.* **2010**, *12*, 7352 – 7365; b) R. van Grondelle, V. I. Novoderezhkin, *Phys. Chem. Chem. Phys.* **2006**, *8*, 793 – 807.

[3] a) Y. Mazor, A. Borovikova, N. Nelson, W. Kuhlbrandt, *eLife* **2015**, *4*, e07433; b) X. Qin, M. Suga, T. Kuang, J. R. Shen, *Science* **2015**, *348*, 989 – 995; c) M. Suga, F. Akita, K. Hirata, G. Ueno, H. Murakami, Y. Nakajima, T. Shimizu, K. Yamashita, M. Yamamoto, H. Ago, J.-R. Shen, *Nature* **2015**, *517*, 99 – 103; d) S. Niwa, L.-J. Yu, K. Takeda, Y. Hirano, T. Kawakami, Z.-Y. Wang-Otomo, K. Miki, *Nature* **2014**, *508*, 228 – 232; e) X. Pan, Z. Liu, M. Li, W. Chang, *Curr. Opin. Struct. Biol.* **2013**, *23*, 515 – 525; f) T. Barros, A. Royant, J. Standfuss, A. Dreuw, W. Kuhlbrandt, *EMBO J.* **2009**, *28*, 298 – 306; g) P. Jordan, P. Fromme, H. T. Witt, O. Klukas, W. Saenger, N. Krausz, *Nature* **2001**, *411*, 909 – 917; h) G. McDermott, S. M. Prince, A. A. Freer, A. M. Hawthornthwaite-Lawless, M. Z. Papiz, R. J. Cogdell, N. W. Isaacs, *Nature* **1995**, *374*, 517 – 521.

[4] a) G. S. Schlau-Cohen, T. R. Calhoun, N. S. Ginsberg, M. Ballottari, R. Bassi, G. R. Fleming, *Proc. Natl. Acad. Sci. USA* **2010**, *107*, 13276 – 13281; b) S. Savikhin in *Photosystem I: The Light-Driven Plastocyanin:Ferredoxin Oxidoreductase* (Ed.: J. H. Golbeck), Springer Netherlands, Dordrecht, **2006**, pp. 155 – 175.

[5] a) J. Adolphs, T. Renger, *Biophys. J.* **2006**, *91*, 2778 – 2797; b) T. Renger, F. Müh, *Phys. Chem. Chem. Phys.* **2013**, *15*, 3348 – 3324; c) V. I. Novoderezhkin, M. A. Palacios, H. van Amerongen, R. van Grondelle, *J. Phys. Chem. B* **2005**, *109*, 10493 – 10504; d) A. Damjanović, H. M. Vaswani, P. Fromme, G. R. Fleming, *J. Phys. Chem. B* **2002**, *106*, 10251 – 10262.

[6] a) G. Renger, J. Pieper, C. Theiss, I. Trostmann, H. Paulsen, T. Renger, H. J. Eichler, F. J. Schmitt, *J. Plant Physiol.* **2011**, *168*, 1462 – 1472; b) T.-C. Dinh, T. Renger, *J. Chem. Phys.* **2015**, *142*, 034104.

[7] D. Bednarczyk, S. Takahashi, H. Satoh, D. Noy, *Biochim. Biophys. Acta Bioenerg.* **2015**, *1847*, 307 – 313.

[8] D. Horigome, H. Satoh, N. Itoh, K. Mitsunaga, I. Oonishi, A. Nakagawa, A. Uchida, *J. Biol. Chem.* **2007**, *282*, 6525 – 6531.

[9] a) J. A. Shelnutt, X.-Z. Song, J.-G. Ma, S.-L. Jia, W. Jentzen, C. J. Medforth, *Chem. Soc. Rev.* **1998**, *27*, 31 – 42; b) K. M. Barkigia, L. Chantranupong, K. M. Smith, J. Fajer, *J. Am. Chem. Soc.* **1988**, *110*, 7566 – 7567.

[10] T. Renger, I. Trostmann, C. Theiss, M. E. Madjet, M. Richter, H. Paulsen, H. J. Eichler, A. Knorr, G. Renger, *J. Phys. Chem. B* **2007**, *111*, 10487 – 10501.

[11] W. Humphrey, A. Dalke, K. Schulten, *J. Mol. Graphics* **1996**, *14*, 33 – 38.

[12] a) B. A. Diner, E. Schlodder, P. J. Nixon, W. J. Coleman, F. Rappaport, J. Lavergne, W. F. J. Vermaas, D. A. Chisholm, *Biochemistry* **2001**, *40*, 9265 – 9281; b) T. Morosinotto, J. Breton, R. Bassi, R. Croce, *J. Biol. Chem.* **2003**, *278*, 49223 – 49229.

[13] a) J. N. Sturgis, B. Robert, *J. Phys. Chem. B* **1997**, *101*, 7227 – 7231; b) J. N. Sturgis, B. Robert, *Photosynth. Res.* **1996**, *50*, 5 – 10; c) H. Witt, E. Schlodder, C. Teutloff, J. Niklas, E. Bordignon, D. Carbonera, S. Kohler, A. Labahn, W. Lubitz, *Biochemistry* **2002**, *41*, 8557 – 8569; d) K. McLuskey, S. M. Prince, R. J. Cogdell, N. W. Isaacs, *Biochemistry* **2001**, *40*, 8783 – 8789.

[14] a) M. O. Senge, S. A. MacGowan, J. M. O'Brien, *Chem. Commun.* **2015**, *51*, 17031 – 17063; b) M. O. Senge, *Chem. Commun.* **2006**, 243 – 256.

[15] a) M. O. Senge, W. W. Kalisch, S. Runge, *Tetrahedron* **1998**, *54*, 3781 – 3798; b) E. Gudowska-Nowak, M. D. Newton, J. Fajer, *J. Phys. Chem.* **1990**, *94*, 5795 – 5801.

[16] a) I. Renge, K. Mauring, *Spectrochim. Acta Part A* **2013**, *102*, 301 – 313; b) T. Renger, B. Grundkötter, M. E.-A. Madjet, F. Müh, *Proc. Natl. Acad. Sci. USA* **2008**, *105*, 13235 – 13240.

[17] a) G. Zucchelli, S. Santabarbara, R. C. Jennings, *Biochemistry* **2012**, *51*, 2717 – 2736; b) G. Zucchelli, D. Brogioli, A. P. Casazza, F. M. Garlaschi, R. C. Jennings, *Biophys. J.* **2007**, *93*, 2240 – 2254.

[18] K. Saito, Y. Umena, K. Kawakami, J.-R. Shen, N. Kamiya, H. Ishikita, *Biochemistry* **2012**, *51*, 4290 – 4299.

[19] S. Jurinovich, C. Curutchet, B. Mennucci, *ChemPhysChem* **2014**, *15*, 3194 – 3204.

[20] S. A. MacGowan, M. O. Senge, *Biochim. Biophys. Acta Bioenerg.* **2016**, *1857*, 427 – 442.

[21] a) R. Remelli, C. Varotto, D. Sandonà, R. Croce, R. Bassi, *J. Biol. Chem.* **1999**, *274*, 33510 – 33521; b) R. Bassi, R. Croce, D. Cugini, D. Sandonà, *Proc. Natl. Acad. Sci. USA* **1999**, *96*, 10056 – 10061; c) E. Wientjes, G. Roest, R. Croce, *Biochim. Biophys. Acta Bioenerg.* **2012**, *1817*, 711 – 717.

Received: December 29, 2015
Revised: February 18, 2016
Published online: April 21, 2016

 © 2016 Wiley-VCH Verlag GmbH & Co. KGaA, Weinheim